Global Assessment of Consistency and Uncertainty in Vegetation Indices from NASA's Harmonized Landsat and Sentinel-2 Project

Qiang Zhou[1,2], Margaret Wooten[1,2], Christopher S.R. Neigh[2], Junchang Ju[2,3], Madhu Sridhar[4], Bradley W Baker[4]

[1]Science Systems and Applications, Inc (SSAI), contractor to NASA GSFC, USA; [2]NASA Goddard Space Flight Center, Maryland, USA; [3]University of Maryland, Maryland, USA; [4]University of Alabama in Huntsville, Huntsville, AL, USA; [5]NASA Marshall Space Flight Center, Martin Rd SW, Huntsville, AL 35808, USA

Abstract

NASA's Harmonized Landsat and Sentinel-2 (HLS) Version 2.0, a global surface reflectance product (excluding Antarctica) derived from Landsat 8/9 and Sentinel-2 A/B/C (L30/S30), became temporally complete in Summer 2023 via LP DAAC, AWS, and GEE. A suite of Vegetation Indices (VIs) derived from HLS V2.0 has recently been released, beneficial for dense time-series vegetation applications. To evaluate the reliability of these VIs, this study examined the between-sensor consistency of VIs derived from HLS V2.0 on a global scale. The evaluation utilizes same-day L30 and S30 image pairs from diverse landscapes around the world. Over 136 million cloud-free pixel pairs were randomly sampled to assess the VI difference between Landsat and Sentinel-2. First, the normalized Root Mean Square Deviation Inter-Quartile Range (RMSDIQR) and R^2 for each VI derived from L30 and S30 were calculated. Second, factors potentially contributing to discrepancies were then investigated. The analysis revealed that large view azimuth angle differences can cause a slight increase in discrepancies between Landsat and Sentinel-2 for some VIs. Similarly, a high solar zenith angle, which occurs during winter, can also result in increased discrepancies for some VIs. Finally, we analyzed VI uncertainties across different VI values and aerosol optical depths. Using VIs derived from low-level aerosols and cloud-free observations as a baseline, we assessed the impact of aerosol levels. VIs derived from moderate-level aerosol conditions closely aligned with the baseline. However, high aerosol levels introduced evident discrepancies, highlighting increased uncertainty in VIs under these conditions. Additionally, even for low-level aerosol observations, low discrepancies were often found within a range of VIs values, while extremely low or high VIs exhibited higher uncertainty. The study provides insights for researchers using these indices for reliable vegetation monitoring and analysis.

Method

Index name	Abbrev.	Equation
Normalized difference vegetation index	NDVI*	$\frac{NIR - Red}{NIR + Red}$
Enhanced vegetation index	EVI*	$2.5 \times \frac{NIR - Red}{NIR + 6 \times Red - 7.5 \times Blue + 1}$
Soil Adjusted Vegetation Index	SAVI*	$1.5 \times \frac{NIR - Red}{NIR + Red + 0.5}$
Modified Soil Adjusted Vegetation Index	MSAVI*	$\frac{2 \times NIR + 1 - \sqrt{(2 \times NIR + 1)^2 - 8 \times (NIR - Red)}}{2}$
Normalized Difference Moisture Index	NDMI*	$\frac{NIR - SWIR1}{NIR + SWIR1}$
Normalized Difference Water Index	NDWI*	$\frac{Green - NIR}{Green + NIR}$
Normalized Burn Ratio	NBR*	$\frac{NIR - SWIR2}{NIR + SWIR2}$
Normalized Burn Ratio 2	NBR2*	$\frac{SWIR1 - SWIR2}{SWIR1 + SWIR2}$
Triangular vegetation index	TVI*	$\frac{120 \times (NIR - Green) - 200 \times (Red - Green)}{2}$
Enhanced vegetation index 2	EVI2	$2.5 \times \frac{NIR - Red}{NIR + 2.4 \times Red + 1}$
Near-infrared reflectance of vegetation	NIRv	$\frac{NIR - Red}{NIR + Red} \times NIR$
kernel NDVI	kNDVI	$tanh(NDVI^2)$
Optimized Soil Adjusted Vegetation Index	OSAVI	$(1 + 0.16) \times \frac{NIR - R}{NIR + R + 0.16}$
Fluorescence Correction Vegetation Index	FCVI	$NIR - (Blue + Green + Red)$
Modified FCVI	FCVI_VIS	$\frac{NIR - (Blue + Green + Red)}{Blue + Green + Red}$
Normalized green red difference index	NGRDI	$\frac{Green - Red}{Green + Red}$
Green leaf index	GLI	$\frac{2 \times Green - Red - Blue}{2 \times Green + Red + Blue}$
Visible atmospherically resistant index	VARI	$\frac{Green - Red}{Green + Red - Blue}$
Ratio vegetation index (also called simple ratio)	RVI	$\frac{NIR}{Red}$
Chlorophyll vegetation index	CVI	$\frac{NIR \times R}{Green^2}$
Chlorophyll index – green	CIG	$\frac{NIR}{Green} - 1$

Table 1. Evaluated vegetation indices.
*available in the HLS VI product

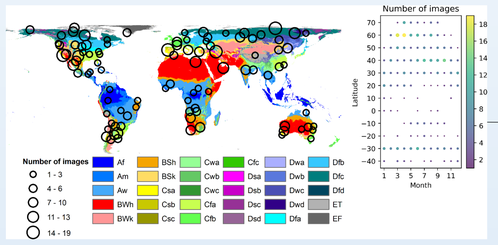

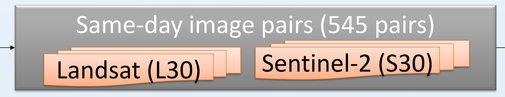

Random sample of cloud-free pairs (~136 million pixels)

$$RMSDIQR = \frac{RMSD}{Q_3 - Q_1} = \frac{\sqrt{\frac{1}{n}\sum_i^n (v_i^t - v_i^s)^2}}{Q_3 - Q_1}$$

Figure 1. Workflow

Results

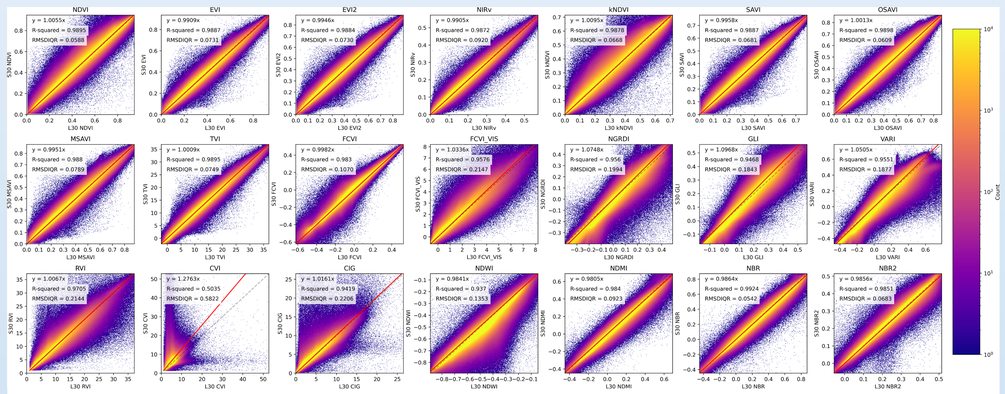

Figure 2. Scatterplots comparing the vegetation indices values derived from HLS L30 (x-axis) and S30 (y-axis). The red solid line represents the reduced major axis (RMA) regression line fixed through the origin, and the dashed line shows1:1 correlation for reference.

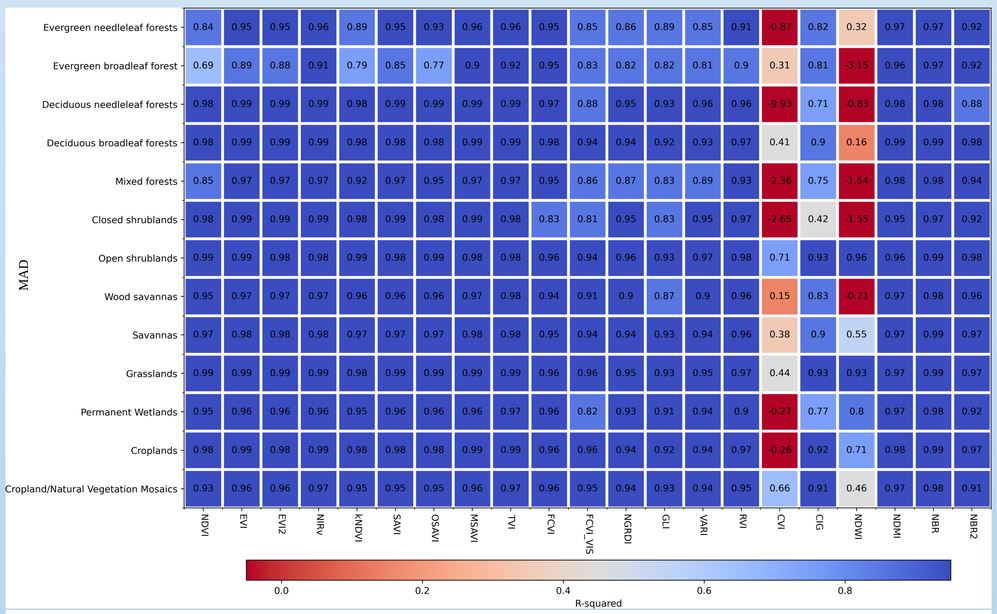

Figure 3. Variations of R-squared between HLS L30 and S30 derived vegetation indices (VI) with respect to the vegetation cover types (MODIS MCD12Q1 Version 6.1) (x-axis).

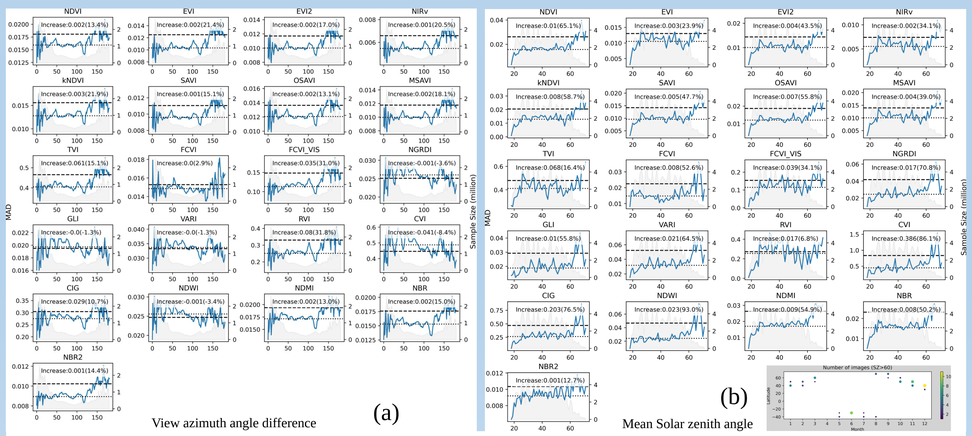

Figure 4. The mean absolute difference (MAD) (blue line, left-hand Y-axis) between HLS L30 and S30 derived vegetation indices (VI) with respect to (a) the view azimuth angle difference (VAD) and (b) the solar zenith angle (SZ) (x-axis). Dotted line represents the average MAD of VAD<125° (or SZ<60°) and the dashed line represents the average MAD of VAD≥125° (or SZ≥60°). The annotation shows the change between two lines and the percentage relative to the dotted line. The histogram (gray shade) shows the sample size with Y-axis on the right.

Results

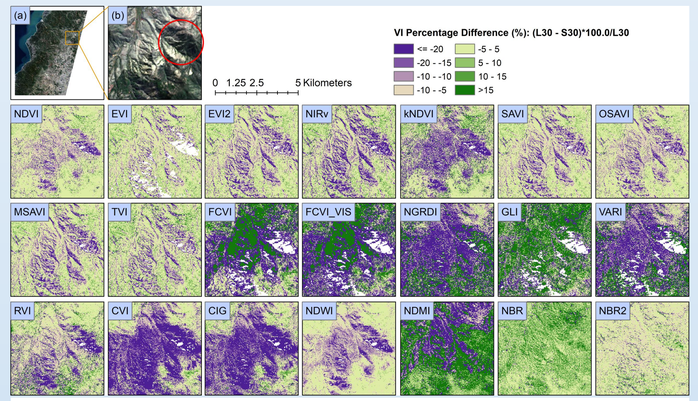

Figure 5. Spatially-explicit VI differences derived from the same-day HLS L30 and S30 in Cancha de Quillay, Chill. (Tile ID: 18HYF, Date: April-28-2022) (a) shows the tile overview in L30 RGB color combination. (b) and the rest panels show the zoom-in area. The red circle in (b) is a shadow area with dense vegetation.

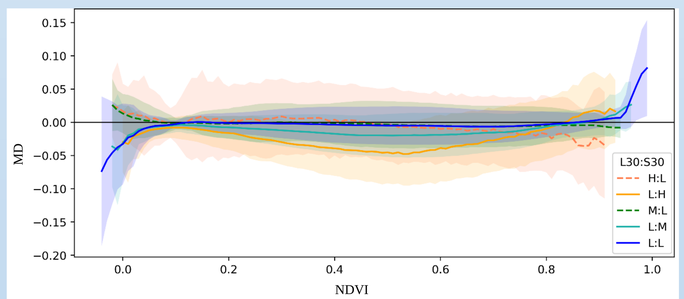

Figure 6. Deviations of VIs for different aerosol level combinations, expressed as the mean difference (MD). The MD is the average difference between values from the L30 and S30 derived VIs, where a positive MD represents a higher VI value derived from L30. The colors represent different combinations of aerosol levels from L30 and S30 where L = low, M = moderate, and H = high. The lines show the mean difference (MD) for different aerosol combinations, and the shadows represent their standard deviation. The horizontal line represents MD=0.

Conclusion

1. Most VIs exhibited high between-sensor consistency, except for a few VIs designed for specific land cover conditions.
2. Large view azimuth angle differences or high solar zenith angle can slightly increase between-sensor discrepancies.
3. VIs derived from high aerosol levels, as indicated by the HLS QA band, exhibit higher discrepancies.
4. Extreme VI values also exhibited increased discrepancies, potentially due to soil background influence or significant noise in areas with very low surface reflectance.

References

Ju, Junchang, et al. "The Harmonized Landsat and Sentinel-2 version 2.0 surface reflectance dataset." *Remote Sensing of Environment* 324 (2025): 114723.

Zhou, Qiang, et al. "Towards Seamless Global 30-meter Terrestrial Monitoring: Evaluating 2022 Cloud Free Coverage of Harmonized Landsat and Sentinel-2 (HLS) V2. 0." *IEEE Geoscience and Remote Sensing Letters* (2025).

Zhou, Qiang, et al. " Global Uncertainty Assessment of Vegetation Indices from NASA's Harmonized Landsat and Sentinel-2 Project " *pub in prep*.

Acknowledgement

For more information please visit: https://hls.gsfc.nasa.gov/

This work is supported by NASA Grant 80GSFC20C0044 and 80MSFC22M004